Int. J. Heat Mass Transfer. Vol. 12, pp. 319–331. Pergamon Press 1969. Printed in Great Britain

A NON-EQUILIBRIUM DESCRIPTION OF TWO-PHASE ANNULAR FLOW

APPLICATION TO THE BURNOUT PREDICTION*

L. BIASI, G. C. CLERICI, R. SALA† and A. TOZZI

A.R.S. S.p.A. and Istituto di Scienze Fisiche dell'Università di Milano, Italy

(*Received* 28 *January* 1968 *and in revised form* 29 *July* 1968)

Abstract—A description is given of a heat-transfer annular dispersed flow in terms of non-equilibrium in the phase distribution. A simple equation relating film flowrate variation to heat flux and to the departure from equilibrium is used to predict the dry-out point in circular ducts. The results obtained are compared with the experimental burnout data for uniform and non-uniform heating.

NOMENCLATURE

C, concentration [g/cm^3];
F, function connected with β by equilibrium equation [dimensionless];
G, specific mass flowrate [g/cm^2 s];
H_{LG}, latent heat of vaporization [J/g];
l, mixing length [cm];
R, duct radius [cm];
S, slip ratio [dimensionless];
V, phase velocity [cm/s];
W, specific mass flux [g/cm^2 s];
z, axial dimension of the channel [cm];
X, quality [dimensionless].

Greek symbols

$\bar{\alpha}$, void fraction [dimensionless];
β, function defined by equation (8) [dimensionless];
ψ, function defined by equation (9) [dimensionless];
χ, numerical constant [dimensionless];
ρ, density [g/cm^3];
τ, shear stress [dyn/cm^2];
ϕ, thermal heat flux [W/cm^2].

Subscripts

D, diffusion;
E, entrainment;
eq, equilibrium;
G, gas;
in, inlet;
l, liquid;
lc, liquid in the core;
lf, liquid in the films;
mc, mean in the core;
o, outlet.

INTRODUCTION

THE KNOWLEDGE of the two-phase behaviour in heat-transfer conditions has become increasingly important in connection with the nuclear reactor design. Different situations can be present according to the type of flow pattern actually existing at present in the mixture. In the present work a theoretical description of an annular dispersed flow with heat addition is presented, in terms of non-equilibrium phenomena in the phase distribution. Following the usual representation, the flow pattern is approximated by an annular film around the duct wall and a central core. Both phases are considered to be present everywhere, but liquid is the prevailing phase in the film, whilst gas is prevailing in the core.

* Work partly supported by Euratom under the contract No. 106-66-12 TEEI(RD) and partly by CNEN—Nuclear Applied Research Division.

† A.R.S. S.p.A.

In adiabatic conditions the liquid film flowrate is constant and the mass-transfer process-core-to-film diffusion of liquid droplets, film-to-core entrainment of liquid lumps have equal rates. In heat-transfer conditions the film flowrate value decreases following the quality local change and, in addition, the whole evaporation being assumed to take place in the film, an excess amount ΔG_{lf} of the liquid flow per unit area is subtracted from the liquid film. This leads to a non-equilibrium phase distribution in which diffusion and entrainment are no longer balanced.

As a first approximation the non-equilibrium effect is described by a simple differential equation in which the mass flux from the core to the film in the direction of equilibrium is assumed to be proportional to ΔG_{lf}. The proportionality factor is deduced by analogy with single phase phenomena, except for an empirically determined arbitrary constant. By integrating this equation, the local film flowrate can be obtained over all the duct length. At each integration step the knowledge of the equilibrium film flowrate corresponding to the local quality is required. This quantity is provided by a model proposed by the authors [1, 2] in which film thickness, liquid film flowrate and mean slip in the core are obtained by solving Von Kármán's equation for a turbulent motion in the film and core, assuming total pressure drop and the mean void fraction $\bar{\alpha}$ as known. Unfortunately not all the solutions can be given in a closed form, and the film flowrate has to be determined by numerically solving a transcendent equation.

The model here presented allows to predict the burnout as liquid film dry-out for every kind of heat flux distribution. Its range of application is restricted to high turbulent symmetric steady flow, with annular dispersed flow pattern. Consequently the only data directly comparable are those obtained with positive inlet quality. An extension to subcooled inlet conditions is also presented by assuming equilibrium vaporization up to the point in which annular dispersed flow is established. A detailed comparison with the experimental burnout data, both for uniform and non-uniform heating, seems to support the validity of the approach here proposed.

1. KINETIC EQUATION

Assuming steady conditions, neglecting the variation of the various quantities due to pressure losses, a fully developed adiabatic annular dispersed flow can be described by a set of equilibrium equations. The typical quantities of the system (film thickness, film flowrate, etc.) depend only on the local values of the variables describing the system itself.

With heat addition the non-equilibrium effects on the phase distribution cannot be neglected and the system local state is the result of the evolution of the initial state which is governed by the rates of heat- and mass-transfer processes. Considering a film flowrate conservation equation, three main processes can be taken into account: evaporation, diffusion, entrainment.

The first one is the direct result of heat addition and its overall effect is described by the heat balance equation provided thermodynamic equilibrium can be supposed to be maintained in the system. In this representation of the flow pattern, this process takes place at the film-core interface and leads to a reduction in the liquid film flowrate. As a result of evaporation, an excess amount of liquid flow is subtracted from the film, therefore the film flowrate is no longer in equilibrium with the system local state.

The second one describes the diffusion of the liquid droplets dispersed in the core towards the wall. This process increases the liquid flowrate in the film and tends to restore equilibrium.

Entrainment is a highly complex phenomenon depending on film velocity fluctuations and on slip ratio between the two phases, which leads to the formation of superficial waves. As a result of this process some liquid lumps, ejected from the film, enter the central gaseous zone. W_H, W_D and W_E being the specific mass fluxes (g/cm^2 s) for evaporation, diffusion, and entrainment processes, the equation describing the specific

liquid film flowrate evolution along the axial dimension Z of a channel can be written as:

$$\frac{dG_{lf}}{dz} = (W_H + W_D - W_E)\frac{2}{R}. \quad (1)$$

Under equilibrium conditions, diffusion and entrainment are not independent, since the equilibrium state is characterized by the equality between the rates of these two processes. Owing to this the knowledge of an analytical expression of only one of these two rates, in addition to the equilibrium solution is sufficient for a complete description of the system. On the other hand, under non-equilibrium conditions, the only available relation is the basic assumption that the process rates must have the same functional dependence on local variables as in equilibrium conditions. According to this basic concept, the following scheme is usually used:

(i) An analytical expression is first obtained of the rate of one of the processes as a function of the system state.
(ii) The remaining velocity is then derived by using the equilibrium solution.
(iii) The obtained expressions are applied to non-equilibrium conditions by using the local values of the variables on which they depend.

In this scheme the knowledge of an analytical form describing the equilibrium state is basic in suggesting the functional dependence of the process rates on the various parameters. The equilibrium solution however allows to determine the expressions of the two rates except for an arbitrary function, which is present in both terms. Unfortunately, as previously remarked, the equilibrium solution is obtained by numerically solving a transcendent equation and therefore its analytical expression cannot be used.

When the system is not very far from equilibrium, it seems reasonable to assume

$$W_D - W_E \simeq \psi(G_{lf_{eq}} - G_{lf}). \quad (2)$$

Actually from a mathematical viewpoint this corresponds to a linearized description of the process, from a physical one to the assumption that relaxation is directly proportional to the departure from equilibrium. The problem is now to obtain the expressions for W_D and W_E. First a theoretical expression of diffusion rate is determined since this process seems to be clearer from a physical viewpoint. As a first approximation diffusion rate was assumed to be proportional to the liquid concentration C_{lc} and to the velocity transversal fluctuation $|\overline{V'}|$ in the core times the ratio ρ_G/ρ_l:

$$W_D \simeq C_{lc}\,|\overline{V'}|\,\rho_G/\rho_l. \quad (3)$$

This term ρ_G/ρ_l is introduced in order take into account the difference between liquid and gas transversal velocity, due to different density.

The liquid concentration in the core can be written as:

$$C_{lc} = \frac{G_{lc}}{u_{lc}} = \frac{G_{lc}\,S_{mc}\,\rho_G}{G_G} \quad (4)$$

where G_{lc} is liquid specific flowrate in the core, G_{lf} liquid specific flowrate in the film, u_{lc} liquid velocity in the core, S_{mc} mean slip ratio in the core, ρ_G gas density and G_G gas specific flowrate.

According to von Kármán's theory [3], the transversal velocity fluctuation in the core is:

$$|\overline{V'}| \sim l\,|\overline{du/dy}| \simeq \sqrt{(\tau/\rho_G)}. \quad (5)$$

The diffusion rate W_D becomes then:

$$W_D = \beta\,\frac{\rho_G^{\frac{3}{2}}\,\tau_c^{\frac{1}{2}}\,S_{mc}\,G_{lc}}{\rho_l\,G_G} \quad (6)$$

τ_c being the film-core interface, and β a function of the local values of the parameters describing the proportionality constant of equation (3) and any other neglected effect.

Now the entrained flux is written as:

$$W_E = F\,\frac{\rho_G^{\frac{3}{2}}\,\tau_c^{\frac{1}{2}}\,S_{mc}\,G_{lf}}{\rho_l\,G_G} \quad (7)$$

where F is a dimensionless function connected with β by the equilibrium equation. This expression was selected being the simplest one

satisfying the boundary condition $W_E \to 0$ when $G_{lf} \to 0$.

As W_E and W_D must satisfy the equilibrium condition and equation (2), one obtains:

$$\beta = F G_{lf_{eq}} / G_{lc_{eq}} \tag{8}$$

$$\psi = \frac{\rho_G^{\frac{1}{2}} \tau_c^{\frac{1}{2}} S_{mc} G_l}{\rho_l G_G G_{lc_{eq}}} F. \tag{9}$$

Owing to the weak dependence of the ratio $G_l/G_{lc_{eq}}$ on the system parameters, in first approximation the dimensionless group $FG_l/G_{lc_{eq}}$ was assumed to be a numerical constant, established in 2·3 by comparing at a preliminary stage a set of experimental burnout measurements with the dry-out predictions of equation (9). No optimization of this coefficient was tried since the main aim of the work was to point out the model capability to predict the correct trend of critical heat flux with the various parameters more than its numerical agreement. With this assumption, equation (1) becomes:

$$\frac{dG_{lf}}{dZ} = -\frac{2\phi}{RH_{lG}} + 4{\cdot}6 \frac{\rho_G^{\frac{1}{2}} \tau_c^{\frac{1}{2}} S_{mc}}{\rho_l G X R} (G_{lf_{eq}} - G_{lf}) \tag{10}$$

or also assuming the quality X as an independent variable

$$\frac{dG_{lf}}{dX} = -G + 2{\cdot}3 \frac{\rho_G^{\frac{1}{2}} \tau_c^{\frac{1}{2}} S_{mc} H_{lG}}{\rho_l \phi X} (G_{lf_{eq}} - G_{lf}). \tag{11}$$

The integration of equation (11) or (10) together with the heat balance equation

$$X = \frac{4}{H_{lG} G D} \int_0^z \phi(l)\, dl + X_{in}$$

give the local film flowrate in an arbitrarily heated duct under the following conditions:

(a) Steady state is achieved over the whole integration field.

(b) The parameters describing the system radius, pressure inlet quality, specific mass flowrate, heat flux distribution and initial local film flowrate $G_{lf}(X_{in})$ are given. A complete equilibrium solution is also required in order to have $G_{lf_{eq}}$, S_{mc} τ_c at every integration step.

2. APPLICATION TO THE BURNOUT PREDICTION

There are several phenomena (thermodynamic non-equilibrium, for instance) which can reduce heat transfer and give rise to burnout before annular dispersed flow is established, but in the high quality region the film dry-out is usually considered as the prevailing phenomenon for the thermal crisis onset. By integrating equation (11), the dry-out point can be determined as the point in which the liquid film flowrate reduces to zero. It can be noted however that the hypothesis, on which equation (11) was based, *a priori* restricts its application to positive inlet conditions. With a fully developed inlet flow, inlet conditions have to be taken equal to those of the corresponding equilibrium. In other cases the inlet conditions can be suggested by the feeding technique of the two-phase mixture. No restrictions are made on the shape of heat flux distribution.

An extension of the presented approach to subcooled inlet conditions (but still with positive outlet) can be performed by assuming that film flowrate depends only on the global parameters and not on the previous history of the channel, at the point where annular dispersed flow is established. In this scheme a change of thermal flux corresponds to a shift of this point, but the phase distribution remains unvaried. This hypothesis is consistent with the analytical form of equation (11) since for low quality ($X \to 0$) the coefficient of $(G_{lf_{eq}} - G_{lf}) \to \infty$ and the solution approaches the equilibrium values whatever the heat flux.

Equation (11) contains two asymptotic solutions representing the extreme cases in which

the coefficient $\rho_G^{\frac{1}{2}} \tau_c^{\frac{1}{2}} S_{mc} H_{lG}/\rho_l \phi X$ goes to ∞ or zero. The former case corresponds to very high diffusion and entrainment rates, the liquid film flowrate thus approaching its equilibrium value in every point. Dry-out occurs therefore at the point $X = 1$. In the latter case evaporation is the only mass-transfer process and the liquid film flowrate decreases linearly. This solution corresponds to very low diffusion and entrainment rates and can be considered as a frozen solution. With a finite value of the coefficient and $G_{lf}(X_{in}) = G_{lf_{eq}}(X_{in})$ at the starting point the solution lies between frozen and equilibrium values.

It must be noted that the solution of equation (11) gives the dry-out point once inlet conditions and heat flux distribution are given. Starting with the experimental value of heat flux, the distance between the inlet and dry-out points is not always equal to the experimental duct length. In order to better compare experimental measurements, an iterative process was introduced, which allowed the predicted dry-out length and the experimental burnout one to coincide, by varying the numerical value of the imposed heat-flux. All the reported results are obtained with this iterative process. The validity of the model here proposed has been tested by comparing the predictions of equation (11) with experimental burnout data for uniform and non-uniform heating, positive and negative inlet conditions. In the former case the transition to annular flow was assumed to occur when the local quality is $X = 0{\cdot}15$. The equilibrium solution required for computations was obtained from reference [1].

3. DISCUSSION OF RESULTS

(a) *Uniform heat flux. Positive inlet conditions*

Report C.I.S.E. R-90 presents a set of experimental burnout measurements obtained with a fully developed inlet flow. The heated section was preceded by a 3·5 m long calming section. The experimental conditions taken into consideration are summarized in Table 1. The adiabatic pressure drop and the average void fraction required by the equilibrium model were calculated by C.I.S.E. correlations [5, 6]. The analysis was restricted to the experimental data satisfying the conditions: $X_{in} > 0{\cdot}15$, in order to have an annular dispersed flow at the inlet, D, G, P in the range in which C.I.S.E. correlations can give satisfactory predictions for Δp and $\bar{\alpha}$. Some of the obtained results are shown in Figs. 1–5. Figure 1 shows the trend of the specific liquid film flowrate as a function of the quality X for the three types of solutions: frozen (dotted line), equilibrium (full line) and non-equilibrium (dashed line) solutions. As it can be clearly seen, the non-equilibrium solution lies between the two other solutions and the dry-out point is very close to the experimental measured burnout outlet quality point. Figure 2 summarizes all the results obtained, subdividing them according to pressure, duct radius and length values. Burnout heat flux experimental values are plotted against the calculated ones and the two dashed lines represent the zone in

Table 1

Reference	P(ata)	L(cm)	D(cm)	G(g/cm^2 s)	X_{in}	X_0	Heat flux distribution
[4]	52	64·5–140	0·807–1·52	110–390	0·12– 0·36	0·28–0·58	uniform
[4]	71	64·5– 80	0·807–1·52	110–390	0·133–0·616	0·25–0·68	uniform
[4]	91	79·8–140	1·52	110–150	0·15– 0·48	0·3 –0·57	uniform
[7]	71	172–556	0·92 –1·26	60–570	−0·46– −0·014	0·2 –0·9	uniform
[4]	71	110	0·5	218	0·21	0·3 –0·5	hot patch (10 cm long)
[13]	70	427	1·26	135–270	−0·1	0·3 –0·5	cold patch (60·5 cm long)
[13]/	70	366	1·26	135–270	−0·28– −0·03	0·28–0·59	stepped inlet peaking (ϕ_{max}/ϕ_{min} = 3·73–2·99–1·91)
[14]	70–108	182	0·976	100–200	−0·45– −0·03	0·28–0·7	stepped chopped cosine

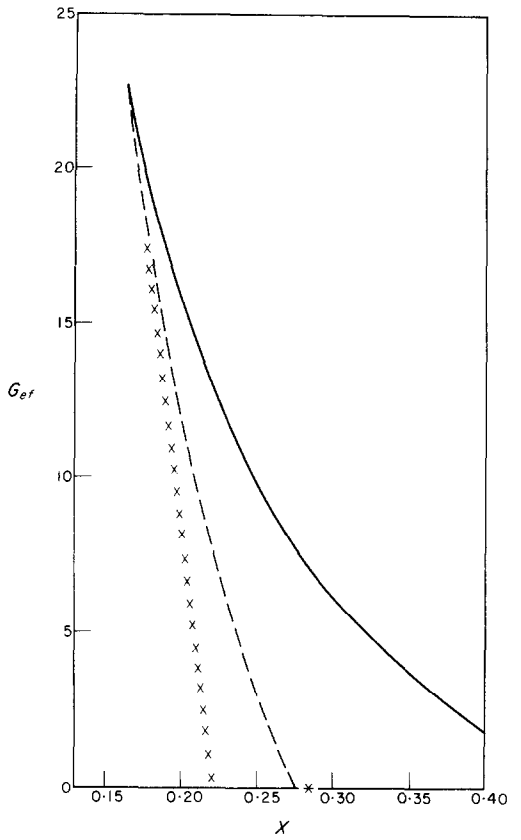

FIG. 1. Trend of G_{lf} as function of X. $-P = 52$ ata, R = 0·4035 cm, $G = 390$ g/cm^2 s, $\phi_{ex} = 230$ W/cm^2.

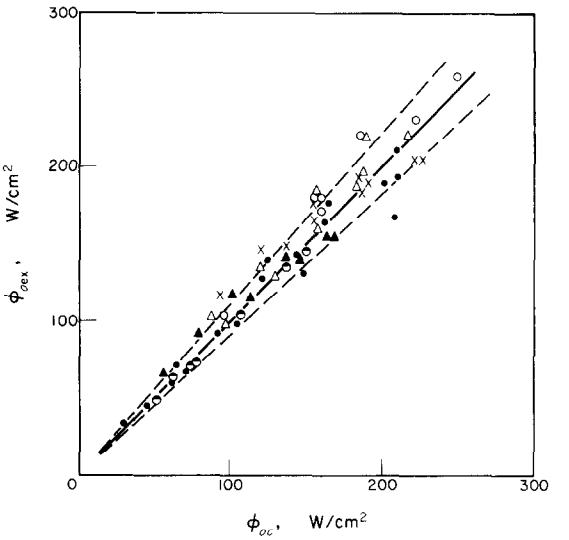

FIG. 2. Experimental values of burnout heat-flux as a function of the calculated ones.

$P = 52$ ata ◓: $R = 0{\cdot}404$ cm, $L = 64{\cdot}5$ cm,
◯: $R = 0{\cdot}459$ cm, $L = 140$ cm,
△: $R = 0{\cdot}76$ cm, $L = 79{\cdot}8$ cm.
$P = 71$ ata ●: $R = 0{\cdot}4035$ cm, $L = 64{\cdot}5$ cm,
×: $R = 0{\cdot}76$ cm, $L = 80$ cm.
$P = 90$ ata ▲: $R = 0{\cdot}76$ cm, $L = 79{\cdot}8$ cm.

which the absolute error is less than 10 per cent. An examination of these figures shows that nearly all the obtained results exhibit an error lower than 10 per cent. A more significant comparison with the experimental results is presented in Figs. 3–5, where total critical power is plotted vs. inlet quality for fixed values of duct radius, mass flowrate and pressure. The predicted critical power trend shows a fairly good agreement with the experimental one both from a qualitative and a quantitative standpoint. Very often the differences lie within the experimental accuracy. It can be noted however that for low mass flowrates ($G \simeq 110$ g/cm^2 is) the predicted values are systematically lower than the experimental ones all over the investigated radius and lengths. At present no attempts were made to improve the mass flowrate dependence. On the other hand it is very difficult to establish whether the error is due to the present model or is introduced by the equilibrium solution through pressure drop and void fraction correlations. Another set of published experimental data with positive inlet conditions [A.E.R.E. R-5072] was not taken into consideration, due to non-equilibrium existing at the channel inlet. Namely the two-phase mixture was produced by mixing subcooled water with superheated steam.

(b) *Uniform heat flux. Subcooled inlet conditions*

A first test of this analysis applicability to burnout prediction with negative inlet quality has been performed by using a set of data reported in [7]. The assumption on which the extension was based leads quite naturally to the exclusion of the data having $X_0 \leqslant 0{\cdot}2$ and

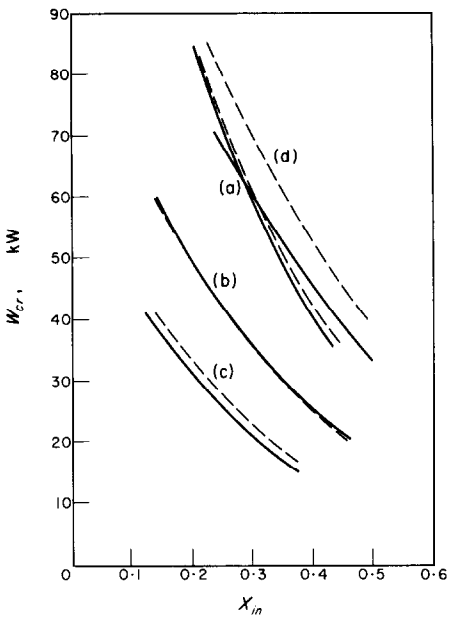

FIG. 3. Trend of the critical power as a function of X_{in}.
$P \cong 52$ ata { (a) $D = 1{\cdot}52$ cm, $L = 80$ cm, $G = 150$ g/cm^2 s; (b) $D = 0{\cdot}918$ cm, $L = 140$ cm, $G = 220$ g/cm^2 s; (c) $D = 0{\cdot}807$ cm, $L = 64{\cdot}5$ cm, $G = 221$ g/cm^2 s; (d) $D = 1{\cdot}52$ cm, $L = 79{\cdot}8$ cm, $G = 110$ g/cm^2 s.

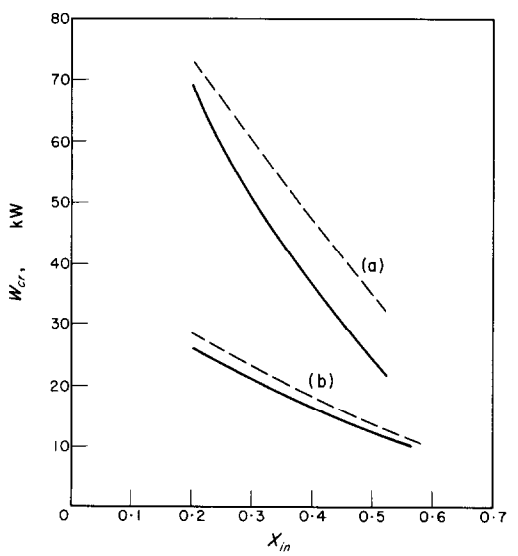

FIG. 4. Trend of the critical power as a function of X_{in}.
$P = 71$ ata { (a) $D = 1{\cdot}52$ cm, $L = 80$ cm, $G = 110$ g/cm^2 s; (b) $D = 0{\cdot}807$ cm, $L = 64{\cdot}5$ cm, $G = 110$ g/cm^2 s.

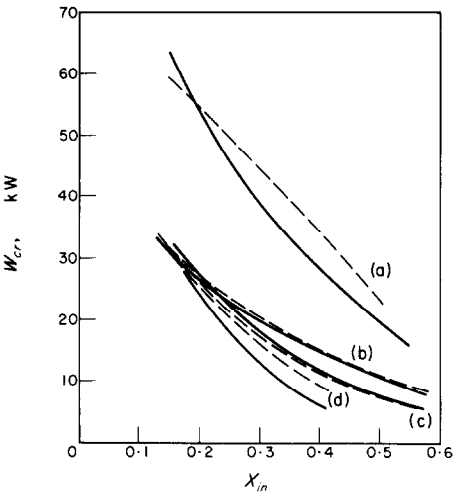

FIG. 5. Trend of the critical power as a function of X_{in}.
$P = 90$ ata { (a) $D = 1{\cdot}52$ cm, $L = 79{\cdot}8$ cm, $G = 110$ g/cm^2 s; (b) $D = 0{\cdot}807$ cm, $L = 64{\cdot}5$ cm, $G = 150$ g/cm^2 s
$P \cong 72$ ata { (c) $D = 0{\cdot}807$ cm, $L = 64{\cdot}5$ cm, $G = 220$ g/cm^2 s; (d) $D = 0{\cdot}807$ cm, $L = 64{\cdot}5$ cm, $G = 390$ g/cm^2 s.

therefore only 135 experimental data, amongst the original 174, have been taken into consideration. The variability range of the involved parameters is also summarized in Table 1. The results seem to be satisfactory, the RMS error over the 135 data being 7·4 per cent. The same group of data has been tested in [7] with four burnout correlations—Harwell [8], Macbeth [9], C.I.S.E. [10], Becker [11]—and in [12] with A.R.S. correlation. The corresponding RMS errors were: 10·1, 11·3, 9·3, 6·7 and 6·5 per cent. As it can be seen, the model prediction presents sometimes a better accuracy than the empirical correlations obtained by fitting experimental data. The error distribution vs. G is shown in Fig. 6: the only systematic error appears at mass flowrate $\lesssim 100$ g/cm^2 s, where the model underpredicts critical heat flux.

(c) *Non-uniform heat flux*

Some experimental burnout measurements with typical nonuniform heat distributions were also compared with the predictions of equation (11).

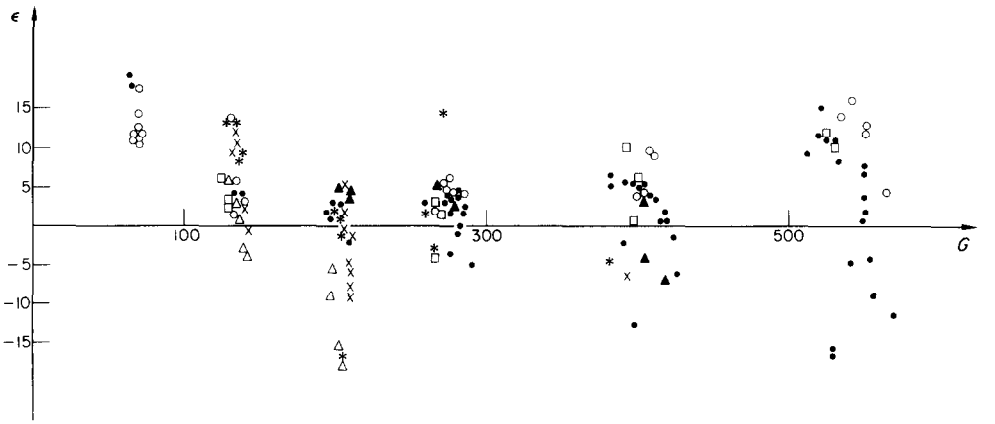

FIG. 6. Error distribution vs. G for data of [7].

First, three sets were selected of data obtained at C.I.S.E. [4] with a test section consisting of two independently heated adjacent parts of different length.

In the first set the short section was towards the inlet whereas in the two others it was towards the outlet.

In all three cases the heated channels were preceded by a 2·5 cm long adiabatic calming section and the crisis was obtained at the outlet by changing the ratio between heat fluxes in the two sections. Computations were carried out for the conditions listed in Table 1, with different heat flux ratios and assuming equilibrium conditions at the inlet. Figure 7 shows the total critical power as a function of the heat flux supplied to the short section (ϕ_2). The continuous lines represent theoretical predictions, and the dashed ones the interpolations of experimental results, marked with dots for the first set and with crosses for the two other. The result dispersion is more apparent than real and is mainly due to the selected representation. Actually in a plot of critical power as a function of heat flux in the long section (ϕ_1), the experimental values are much closer to the predicted ones.

With the short section at the inlet (curves 1), the total critical power is shown to increase monotonously up to a limiting point (c) corresponding to a quasi dry-out conditions. A further increase in ϕ_2 leads to dry-out at the end of the

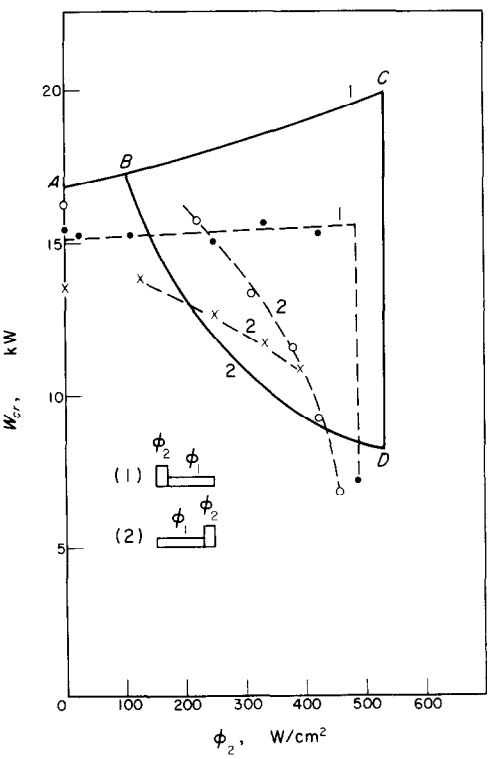

FIG. 7. Critical power input as a function of heat-flux ϕ on short section.

first section and power drops down to the critical value of a 9·4 cm long tube (D). This trend seems physically reasonable since power must increase from point A ($\phi_2 = 0$), representing the critical value of 99·3 cm long tube, to point $B(\phi_1 = \phi_2)$, in which the system is equivalent to a uniformly heated, 108·7 cm long, unique section.

Between B and C, the heat flux ratio is higher than 1 and the power increase can be related to the relaxation of the non-equilibrium phase distribution created in the first section. The latter phenomenon can be clearly seen in Fig. 8,

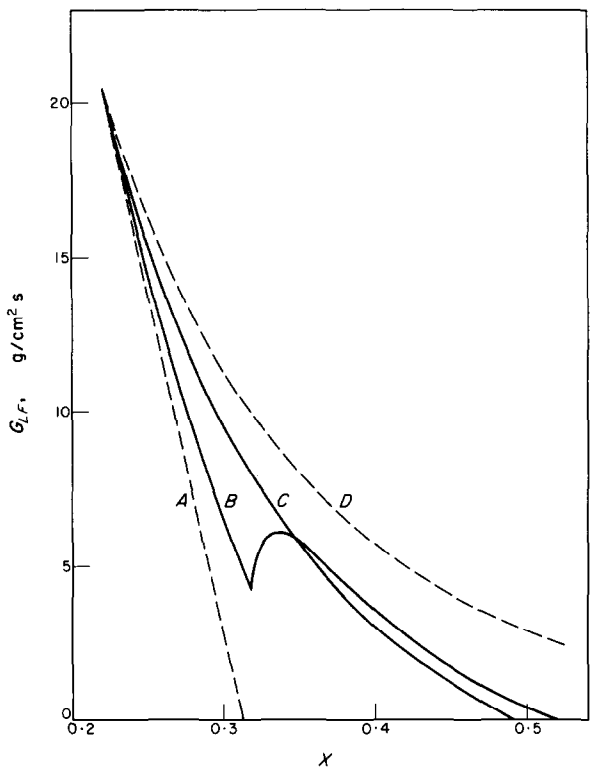

FIG. 8. Film flowrate as a function of the local quality x.

where the liquid film flowrate is plotted as a function of local quality. Curves A and D represent the frozen and equilibrium solutions, curve B is related to heat flux ratio higher than 1 ($\phi_2/\phi_1 \simeq 5$) and curve C is the solution when the two sections are equally heated. Whereas the three solutions A, C and D show a monotonously decreasing trend, the case B presents an inversion at the first section end, due to a net gain of the diffusion process which is no longer balanced by evaporation, owing to heat flux reduction.

When the short section is placed towards the outlet, Fig. 7—curves 2, critical power decreases continuously from point B ($\phi_1 = \phi_2$) to point $D(\phi_1 = 0)$.

For heat flux ratio lower than 1 ($A \leqslant \phi_2 < B$), the solution of equation (11) does not reach the dry-out crisis in the experimental channel length. In this case the long section behaves as a hot patch, the trend of the solution being similar to the one described by curve B of Fig. 8, but the cold section is now too short to reach dry-out before the tube end.

Figure 9 shows, together with the frozen solution (curve A) and the equilibrium solution (curve E), the trend of the film flowrate as a function of the local quality X for some different

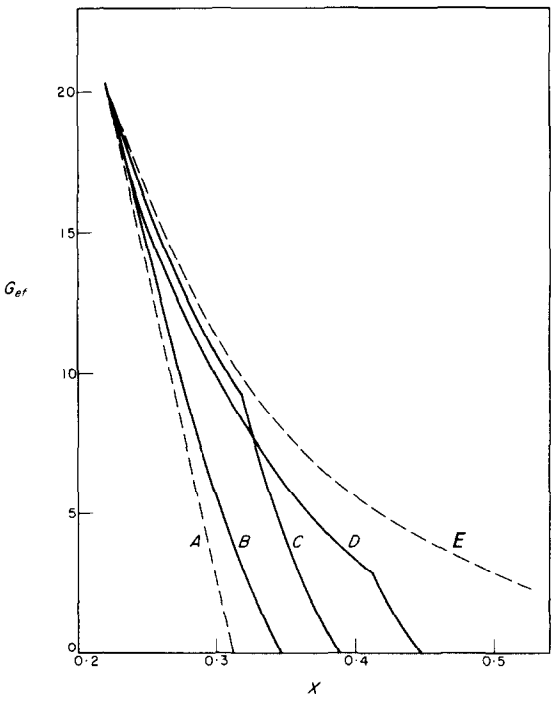

FIG. 9. Film flowrate as a function of the local quality x.

heating conditions. When both sections are heated—curves C and D—the derivatives of the film flowrate with respect to quality present a discontinuity because of the sudden heat-flux variation. By increasing heat flux in the larger section, i.e. going from curve C to D, the non-equilibrium effect increases in this region as well as quality variation. On the other hand in order to have dry-out in the same total length, heat flux and quality change in the short length decrease. The total power input is mainly affected by heat flux in the long section and therefore increases. The minimum power input is obtained with curve B of Fig. 9 and as previously said corresponds to the critical power for a 9·7 cm long tube. The overall agreement with these sets of experimental results can be considered as satisfactory if the slight different inlet conditions and the scattering of the results themselves are taken into account.

The typical behaviour shown by some experimental measurements performed at Harwell [13] with a 60·5 cm long cold patch placed in various positions along a 427 cm long test section was also compared with the solutions of equation (11).

These experiments pointed out a critical power increase above the corresponding value of a uniformly heated tube with the same heated length, when the cold patch is placed towards the exit. In Fig. 10 the experimental and calculated burnout powers are plotted vs. the position of the cold patch start for the inlet conditions: $P = 70$ ata, $D = 1{\cdot}26$ cm, $X_{in} = -0{\cdot}1$, $G = 135$ and 270 g/cm^2 s. The agreement is fairly good and in accordance with the previous discussion. Namely, when the unheated zone is towards the exit, at the cold patch beginning the film is nearly exhausted. Under these conditions the redeposition caused by the unheated zone requires an additional amount of power in order to reach dry-out at the outlet and, therefore, critical power increases. Placing the cold patch quite near the exit, a position marked with A in Fig. 10 is reached, beyond which crisis cannot occur at the duct outlet, but only at the end of the

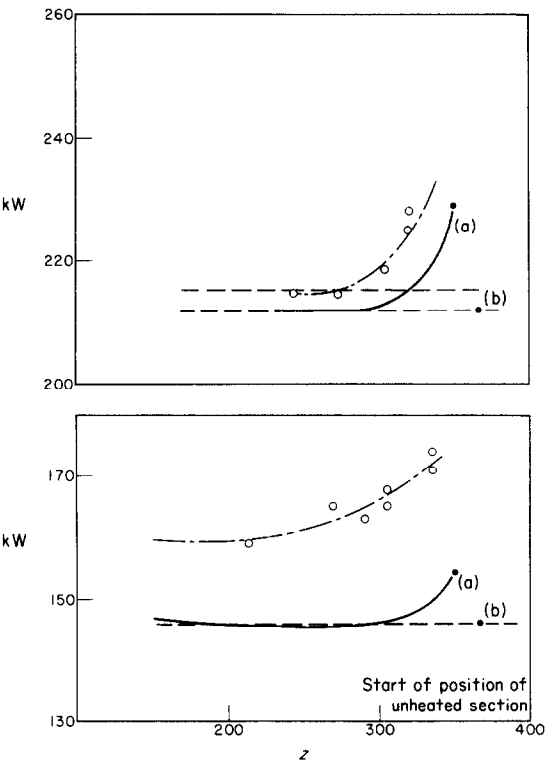

FIG. 10. Burnout power vs. quality at the start of cold patch. $P = 70$ ata $D = 1{\cdot}26$ cm $x_{in} = -0{\cdot}1$ Heated length = 366 cm. $G = \begin{cases} 135 \text{ g/cm}^2 \text{ s} \\ 270 \text{ g/cm}^2 \text{ s.} \end{cases}$

first heated zone. This happens because the heat flux, sufficient to dryout the redeposited film within the duct length being the same on both heated zones, it exhausts the film before the cold patch position. Finally, burnout with an inlet peaking or a chopped cosine heat flux distribution has been considered. The data, taken from [13, 14] are compared with the calculated dry-out points in Figs. 11 and 12 (only the data with $X_0 \gtrsim 0{\cdot}2$ have been considered). With non-uniform heating the first crisis position may be different from the duct and therefore these two quantities are to be predicted by the model: critical heat flux and burnout location. For the inlet peaking the model gives always an outlet burnout: in Fig. 11 the points marked with crosses are those for which also experimental

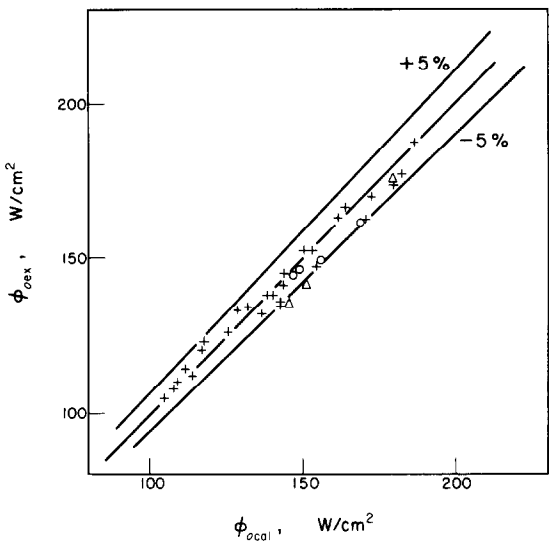

FIG. 11. Critical experimental heat flux vs. the calculated one —chopped cosine.

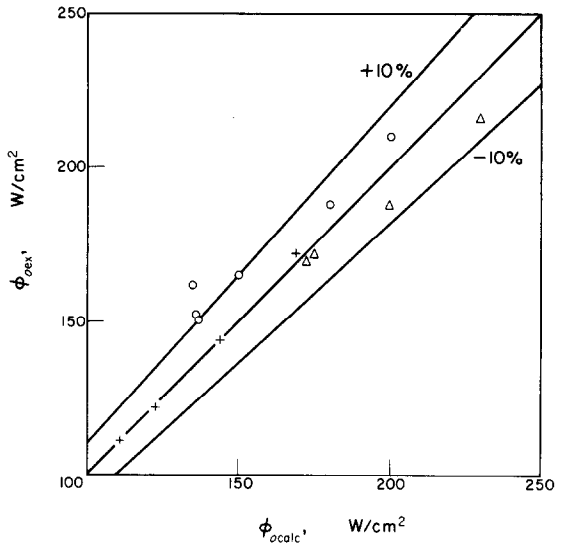

FIG. 12. Critical heat flux vs. the calculated one—inlet peaking.

burnout location is at the exit. Reference [13] shows a transition region between a low quality burnout ($X_0 \sim 0{\cdot}1$ and therefore not described by the present model) located at a 120 cm distance from the inlet and the high quality downstream burnout. For experimental conditions within this region burnout was sometimes determined at the outlet and sometimes at a 240 cm from the inlet.

These few points are marked with triangles ($\phi_{max}/\phi_{min} = 3{\cdot}73$) and circles ($\phi_{max}/\phi_{min} = 2{\cdot}99$). Also for these points the predictions are satistory, in spite of the difference in burnout location. Moreover, according to the model, the last part of the channel is near dry-out and a little heat flux increase (~ 10 per cent) is sufficient to give the coincidence in burnout location. A better agreement was obtained with the data pertinent to chopped cosine heat flux distribution [14]. Here the comparison was made by imposing the coincidence of the first burnout location. This condition has been satisfied for all the examined data. In all cases the model agrees also with the experimental burnout extension, the eventually presented maximum shift being within heat flux step extension (10 cm long). The results are given in Fig. 12 where experimental burnout heat fluxes are plotted vs. the predicted ones.

CONCLUDING REMARKS

An analytical description has been presented of an annular dispersed two-phase flow with heat addition based on non-equilibrium in phase distribution.

An equation describing the film flowrate evolution has been derived and applied to determining burnout heat flux and location point. The numerical agreement with the experimental results both for uniform and non-uniform heating seems to support the approach here proposed in spite of the simplifications introduced.

Nevertheless, in the authors opinion, the main result is the correct prediction of the critical heat flux trend when discontinuities such as cold and hot patches present. The main aim of the present analysis was an analytical description of thermal crisis in the quality region and therefore a right description of deposition and entrainment is beyond its limits. However, some rough information on the deposition rate can be easily obtained by equation (10) by letting

$dG_{lf}/dZ = G_{lf} = 0$. Thus the resulting heat flux ϕ represents the flux for which the local evaporation rate is balanced by the droplet deposition rate. An over and under estimation of the latter quantity can be made by using the initiation flux values and the crisis end in experiments with upstream burnout [13]. In Fig. 13 the deposition rates predicted by the

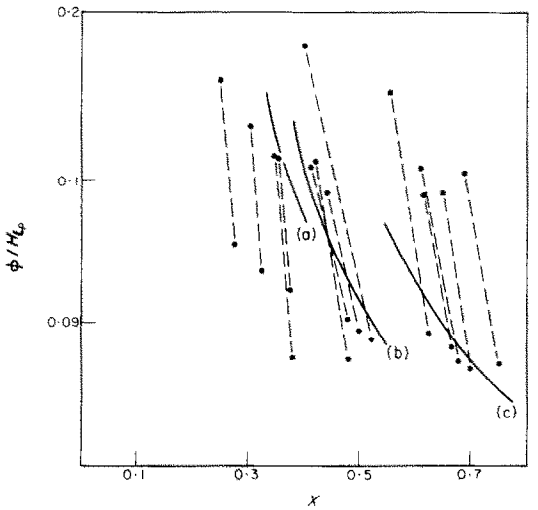

FIG. 13. Deposition rate as a function of quality x.

model are plotted (full line) as a function of quality, together with the limits determined in [14]. Taking into account the difficulty in measuring the extension of an upstream burnout, this further test gives another support to the present analysis.

REFERENCES

1. L. BIASI, G. C. CLERICI, R. SALA and A. TOZZI: A theoretical approach to the Analysis of an adiabatic two phase annular dispersed flow, *Energia Nucl., Milano* **15**, 6, 394–405 (1968).
2. L. BIASI, G. C. CLERICI, R. SALA and A. TOZZI, Studies on film thickness and velocity distribution of two phase annular flow, *Eurat. Rept.* 3765 e (1968).
3. H. SCHLICHTING, *Boundary Layer*, Chapter X. McGraw-Hill, New York (1960).
4. S. BERTOLETTI, G. P. GASPARI, C. LOMBARDI, G. SOLDAINI and R. ZAVATARELLI, Heat transfer crisis in steam–water mixtures. Experimental data in round tubes and vertical upflow obtained during the CAN–2 program, C.I.S.E. R-90 (June 1967).
5. G. P. GASPARI, C. LOMBARDI, G. PETERLONGO, Pressure drops in steam–water mixtures, C.I.S.E. R-83 (1964).
6. P. ALIA, L. CRAVAROLO, A. HASSID and E. PEDROCCHI, Liquid volume fraction in adiabatic two-phase vertical upflow round conduit, C.I.S.E. R-105 (1965).
7. A. W. BENNET, G. R. HEWITT, H. A. KEARSEY and R. K. KEEYS, Measurements of burnout heat flux in uniformly heated round tubes at 1000 psia, AERE R-5055 (1965).
8. G. F. HEWITT, A method of representing burnout data in two-phase heat transfer for uniformly heated round tube, AERE R-4615 (1964).
9. R. V. MACBETH, Burnout analysis. Part IV. Application of a local condition hypothesis to world data for uniformly heated round tubes and rectangular channels, AEEW R-267 (1964).
10. S. BERTOLETTI, G. P. GASPARI, C. LOMBARDI, G. PETERLONGO, M. SILVESTRI and F. TACCONI, Heat-transfer crisis with steam–water mixtures, *Energia Nucl., Milano* **12**, 121 (1965).
11. K. M. BECKER, Some remarks on correlating the Harwell round tube burnout data, AE-RTL-855 (1966).
12. L. BIASI, G. C. CLERICI, S. GARRIBA, R. SALA and A. TOZZI, A new correlation for round ducts and uniform heating, and its comparison with world data, *Energia Nucl., Milano* **14**, 9 530–537 (1967).
13. A. W. BENNET, G. F. HEWITT, H. A. KEARSEY, R. F. KEEYS and D. J. PULLING, Studies of burnout in boiling heat transfer, *Trans. Instn Chem. Engrs* **45** (8) 319–333 (1967).
14. D. H. LEE and J. D. OBERTELLI, An experimental investigation of forced convection burnout in high pressure water. Part II. Preliminary results for round tubes with non-uniform axial heat flux distribution, AEEW R-309 (1963).

Résumé—On décrit le transport de chaleur pour un écoulement annulaire dispersé sous la forme d'un déséquilibre dans la distribution des phases. Une équation simple reliant la variation du débit dans le film au flux de chaleur et à la déviation à partir de l'équilibre est employée pour prédire le point de dessèchement dans les conduits circulaires. Les résultats obtenus sont comparés avec les résultats expérimentaux de "coup de feu" pour un chauffage uniforme et non-uniforme.

Zusammenfassung—Eine Ringströmung eines dispersen wärmeträgers wird mit Methoden des Nichtgleichgewichts in der Phasenverteilung untersucht. Eine einfache Gleichung, die den Einfluss der Änderung des Filmstromes auf den Wärmestrom und das Abweichen vom Gleichgewicht angibt wird verwendet, um den Durchbrennpunkt in ringförmigen Leitungen vorauszubestimmen. Die erhaltenen Ergebnisse werden mit experimentellen Daten für die Siedekrisis bei gleichförmiger und ungleichförmiger Bezeizung verglichen.

Аннотация—С учётом неравновесности фазового распределения дается описание течения в кольцевом канале с теплообменом. Для расчета точки высыхания в кольцевых каналах использовано простое уравнение, содержащее отношение изменения скорости течения пленки к тепловому потоку и к отклонению от состояния равновесия. Полученные результаты сравнивались с экспериментальными данными для однородного и неоднородного нагрева.